Faculty Bibliography 2010s   Faculty Bibliography

1-1-2013

Measurements of the group delay and the group delay dispersion with resonance scanning interferometer

M. K. Trubetskov

M. Von Pechmann

I. B. Angelov

K. L. Vodopyanov
University of Central Florida

F. Krausz

See next page for additional authors

University of Central Florida

STARS
Showcase of Text, Archives, Research & Scholarship

Authors

M. K. Trubetskov, M. Von Pechmann, I. B. Angelov, K. L. Vodopyanov, F. Krausz, and V. Pervak

Measurements of the group delay and the group delay dispersion with resonance scanning interferometer

M. K. Trubetskov,[1,2,*] M. von Pechmann,[4] I. B. Angelov,[1] K. L. Vodopyanov,[3] F. Krausz,[1,4] and V. Pervak[4, 5]

[1]*Max-Planck Institute of Quantum Optics, Hans-Kopfermann 1, 85748 Garching, Germany*
[2]*Research Computing Center, Moscow State University, Leninskie Gory, 119992 Moscow, Russia*
[3]*Univ. Central Florida, CREOL, College of Optics & Photonics, Orlando, FL 32816, USA*
[4]*Ludwig-Maximilians-Universitaet Muenchen, Am Coulombwall 1,85748 Garching, Germany*
[5]*Ultrafast Innovations GmbH Am Coulombwall 1, 85748 Garching, Germany*
[*]*Michael.Trubetskov@mpq.mpg.de*

Abstract: We developed a method for group delay and group delay dispersion measurements, based on location of interference resonance peaks. Such resonance peaks can be observed in transmittance or in reflectance when two mirrors are placed parallel to each other and separated by a thin air spacer. By using a novel approach, based on simultaneous processing of the data acquired for different spacer distances we obtained reliable results with high resolution. Measurements were performed both in transmittance and reflectance layouts depending on the reflectivity of the mirror to be measured. The developed method allows dispersion measurements of ultraviolet mirrors and ultra-broadband mirrors spanning more than one optical octave to be performed.

©2013 Optical Society of America

OCIS codes: (320.7100) Ultrafast measurements; (320.5520) Pulse compression; (310.1620) Interference coatings.

References and links

1. R. Szipöcs, K. Ferencz, C. Spielmann, and F. Krausz, "Chirped multilayer coatings for broadband dispersion control in femtosecond lasers," Opt. Lett. **19**(3), 201–203 (1994).
2. R. Szipőcs and A. Köházi-Kis, "Theory and design of chirped dielectric laser mirrors," Appl. Phys. B **65**(2), 115–135 (1997).
3. J.-C. Diels and W. Rudolph, *Ultrashort laser pulse phenomena : fundamentals, techniques, and applications on a femtosecond time scale* (Academic Press, 1996).
4. D. Strickland and G. Mourou, "Compression of amplified chirped optical pulses," Opt. Commun. **56**(3), 219–221 (1985).
5. A. Ashkin, G. Boyd, and J. Dziedzic, "Resonant optical second harmonic generation and mixing," IEEE J. Quantum Electron. **2**(6), 109–124 (1966).
6. F. X. Kärtner, U. Morgner, R. Ell, T. Schibli, J. G. Fujimoto, E. P. Ippen, V. Scheuer, G. Angelow, and T. Tschudi, "Ultrabroadband double-chirped mirror pairs for generation of octave spectra," J. Opt. Soc. B **18**(6), 882–885 (2001).
7. V. Pervak, A. V. Tikhonravov, M. K. Trubetskov, S. Naumov, F. Krausz, and A. Apolonski, "1.5-octave chirped mirror for pulse compression down to sub-3 fs," Appl. Phys. B **87**(1), 5–12 (2007).
8. V. Pervak, I. Ahmad, M. K. Trubetskov, A. V. Tikhonravov, and F. Krausz, "Double-angle multilayer mirrors with smooth dispersion characteristics," Opt. Express **17**(10), 7943–7951 (2009).
9. V. Pervak, O. Pronin, O. Razskazovskaya, J. Brons, I. B. Angelov, M. K. Trubetskov, A. V. Tikhonravov, and F. Krausz, "High-dispersive mirrors for high power applications," Opt. Express **20**(4), 4503–4508 (2012).
10. V. Pervak, M. K. Trubetskov, and A. V. Tikhonravov, "Robust synthesis of dispersive mirrors," Opt. Express **19**(3), 2371–2380 (2011).
11. M. Trubetskov, A. Tikhonravov, and V. Pervak, "Time-domain approach for designing dispersive mirrors based on the needle optimization technique. Theory," Opt. Express **16**(25), 20637–20647 (2008).
12. M. K. Trubetskov, V. Pervak, and A. V. Tikhonravov, "Phase optimization of dispersive mirrors based on floating constants," Opt. Express **18**(26), 27613–27618 (2010).
13. A. V. Tikhonravov, M. K. Trubetskov, T. V. Amotchkina, and A. A. Tikhonravov, "Application of advanced optimization concepts to the design of high quality optical coatings," Proc. SPIE **4829**, 1061–1062 (2003).
14. O. Nohadani, J. R. Birge, F. X. Kärtner, and D. J. Bertsimas, "Robust chirped mirrors," Appl. Opt. **47**(14), 2630–2636 (2008).

15. J. R. Birge, F. X. Kärtner, and O. Nohadani, "Improving thin-film manufacturing yield with robust optimization," Appl. Opt. **50**(9), C36–C40 (2011).
16. V. Pervak, M. K. Trubetskov, and A. V. Tikhonravov, "Robust synthesis of dispersive mirrors," Opt. Express **19**(3), 2371–2380 (2011).
17. T. V. Amotchkina, M. K. Trubetskov, V. Pervak, B. Romanov, and A. V. Tikhonravov, "On the reliability of reverse engineering results," Appl. Opt. **51**(22), 5543–5551 (2012).
18. W. H. Knox, N. M. Pearson, K. D. Li, and C. A. Hirlimann, "Interferometric measurements of femtosecond group delay in optical components," Opt. Lett. **13**(7), 574–576 (1988).
19. W. H. Knox, "Dispersion measurements for femtosecond-pulse generation and applications," Appl. Phys. B **58**(3), 225–235 (1994).
20. A. Gosteva, M. Haiml, R. Paschotta, and U. Keller, "Noise-related resolution limit of dispersion measurements with white-light interferometers," J. Opt. Soc. B **22**(9), 1868–1874 (2005).
21. M. Beck and I. A. Walmsley, "Measurement of group delay with high temporal and spectral resolution," Opt. Lett. **15**(9), 492–494 (1990).
22. T. V. Amotchkina, A. V. Tikhonravov, M. K. Trubetskov, D. Grupe, A. Apolonski, and V. Pervak, "Measurement of group delay of dispersive mirrors with white-light interferometer," Appl. Opt. **48**(5), 949–956 (2009).
23. K. Naganuma, K. Mogi, and H. Yamada, "Group-delay measurement using the Fourier transform of an interferometric cross correlation generated by white light," Opt. Lett. **15**(7), 393–395 (1990).
24. S. Diddams and J.-C. Diels, "Dispersion measurements with white-light interferometry," J. Opt. Soc. Am. B **13**(6), 1120–1129 (1996).
25. E. Goulielmakis, M. Schultze, M. Hofstetter, V. S. Yakovlev, J. Gagnon, M. Uiberacker, A. L. Aquila, E. M. Gullikson, D. T. Attwood, R. Kienberger, F. Krausz, and U. Kleineberg, "Single-Cycle Nonlinear Optics," Science **320**(5883), 1614–1617 (2008).
26. I. Pupeza, T. Eidam, J. Rauschenberger, B. Bernhardt, A. Ozawa, E. Fill, A. Apolonski, T. Udem, J. Limpert, Z. A. Alahmed, A. M. Azzeer, A. Tünnermann, T. W. Hänsch, and F. Krausz, "Power scaling of a high-repetition-rate enhancement cavity," Opt. Lett. **35**(12), 2052–2054 (2010).
27. V. Pervak, C. Teisset, A. Sugita, S. Naumov, F. Krausz, and A. Apolonski, "High-dispersive mirrors for femtosecond lasers," Opt. Express **16**(14), 10220–10233 (2008).
28. V. Pervak, I. Ahmad, S. A. Trushin, Z. Major, A. Apolonski, S. Karsch, and F. Krausz, "Chirped-pulse amplification of laser pulses with dispersive mirrors," Opt. Express **17**(21), 19204–19212 (2009).
29. O. Pronin, J. Brons, C. Grasse, V. Pervak, G. Boehm, M.-C. Amann, V. L. Kalashnikov, A. Apolonski, and F. Krausz, "High-power 200 fs Kerr-lens mode-locked Yb:YAG thin-disk oscillator," Opt. Lett. **36**(24), 4746–4748 (2011).
30. K. Osvay, G. Kurdi, J. Hebling, A. P. Kovács, Z. Bor, and R. Szipöcs, "Measurement of the group delay of laser mirrors by a Fabry-Perot interferometer," Opt. Lett. **20**(22), 2339–2341 (1995).
31. H. A. Macleod, *Thin-film optical filters* (Taylor & Francis, 2010).
32. D. R. Austin, T. Witting, and I. A. Walmsley, "High precision self-referenced phase retrieval of complex pulses with multiple-shearing spectral interferometry," J. Opt. Soc. Am. B **26**(9), 1818–1830 (2009).
33. A. N. Tikhonov and V. I. Arsenin, *Solutions of Ill-Posed Problems* (Halsted Press, 1977).
34. A. N. Tikhonov, A. Goncharsky, V. V. Stepanov, and A. G. Yagola, *Numerical Methods for the Solution of Ill-posed Problems*, Mathematics and Its Applications No. 328 (Kluwer Academic Publishers, 1995).
35. J. H. Ahlberg, E. N. Nilson, and J. L. Walsh, *The theory of splines and their applications* (Academic Press, 1967).

1. Introduction

Dispersive mirrors (DM) [1–3] are nowadays widely used for precise dispersion control in a broad variety of ultrafast optical devices including femtosecond lasers [3], chirped pulse amplifiers (CPA) [4] and enhancement cavities [5]. DMs are often used in complementary pair configurations [6,7] and in double-angle schemes [8] in order to achieve the smallest possible residual group delay (GD) and group delay dispersion (GDD) oscillations in a broader spectral range.

Due to inevitable manufacturing errors the produced DMs have GD and GDD characteristics that usually deviate from the theoretical design. This problem cannot be avoided even with most modern layer deposition technologies providing sub-nanometer accuracy, since GD and especially GDD are extremely sensitive to deviations in the layer thicknesses of DMs [9,10]. Special design methods including time-domain optimization [11], phase optimization with floating constants [12], based on sensitivity penalty function [13], semi-heuristic approaches [14,15], robust synthesis [16] are able to decrease the sensitivity of DMs to manufacturing errors, but are unable to remove it completely. Therefore accurate measurements of GD and GDD characteristics play crucial role in achieving top performance of ultra-fast optical systems relying on DMs. Additionally, GD and GDD measurements of the produced DMs may provide valuable information for reverse engineering [17], i.e.,

feedback to the manufacturing process in order to further increase the accuracy of the production.

Currently GD and GDD measurements are typically performed with white-light interferometers (WLI) [18–21]. Usually WLI is a Michelson-type interferometer, where measurements are based on changing the length of the reference arm with respect to the length of the arm containing the sample to be characterized. The output signal versus delay (interferogram) is recorded as a function of mean delay (varied step by step) and followed by a specialized data processing in order to retrieve GD and GDD of the sample. Since interferograms are affected by the noise within the light source and the detector as well as by precision of the step motor that is used to change the distance in one of the arms [22], the problem of GD and GDD evaluation is non-trivial and has been considered in several works [18–20,22–24]. Additionally, preliminary alignment of WLI is rather complicated and time-consuming. The resolution in terms of wavelength and/or GDD is often insufficient, especially for demanding applications, such as compression of near-single-cycle optical pulses [25], enhancement cavities requiring mirrors with low dispersion [26], or high-energy oscillators requiring DMs with extremely high values of GDD [9,27–29].

An alternative method for GD and GDD measurements based on detection of interference resonance positions in the inter-mirror spacer was proposed by Osvay *et al* in [30]. Sharp interference resonance peaks are observed in transmittance or in reflectance when two mirrors are placed parallel to each other and separated by a thin air spacer. In [30] GD was obtained on the basis of a formula connecting positions of adjacent resonance peaks and an average GD on the frequency interval between them. This simple approach has a significant disadvantage: for small spacer thickness the distances between resonance peaks are large and this approach has poor frequency resolution. If one increases the spacer thickness in order to improve the resolution, the amplitudes of resonance peaks decrease rapidly and quite soon the peaks cannot be detected in the presence of measurement noise. A "golden middle" spacer thickness is often unable to provide a good balance between resolution and signal-to-noise ratio, especially in the cases of ultra-broadband DMs and high-dispersive DMs. An additional problem of the original approach described in [30] is connected with the necessity of spacer thickness evaluation. It was performed in [30] on the basis of *a priori* information on the measured mirrors, i.e., by using the wavelengths of transmittance maxima in the region where zero GDD was expected. Such additional information is not always available or possible to use.

We propose a more sophisticated approach which provides higher resolution in both frequency and GD domains. It is based on a series of measurements of the resonance peak positions for different spacer thicknesses and consequent simultaneous processing of all obtained information. For brevity we call this approach a *Resonance Scanning Interferometer* (RSI) technique. One of its advantages is that it does not require a precise setting of the spacer thickness or its determination. The only essential requirement is the proper parallel alignment of mirrors and its stability during the entire measurement process. With this improvement, RSI compares favorably with WLI in terms of simplicity/compactness and provides superior accuracy of the GD/GDD measurements.

In Section 2 we consider the theoretical background and basic equations required for the implementation of our method. In Section 3 the measurements layout is described in detail together with advanced data processing algorithm. In Section 4 we show four examples of DM measurements illustrating advantages of the proposed approach.

2. Theory and implementation

Consider two parallel mirrors separated by air (Fig. 1). The characteristics of one of them are known, for our particular purposes we used a metal mirror with GD close to zero [18] and reflectance of about 90%. The second mirror is the sample to be measured, it can be a relatively narrow-band mirror with high value of dispersion and extremely high reflectance (>99.95%) or a broad-band mirror with relatively low value of dispersion and somewhat lowered reflectance (about 98-99.5%). The distance between mirrors in Fig. 1 is exaggerated.

The properties of the sample mirror can be measured in two different layouts: (i) in transmission mode and (ii) in reflection mode, sketched in panel (a) and (b) of Fig. 1, and resembling a Fabry-Perot and Gires-Tournois interferometric setup, respectively. In both cases it is possible to perform measurements at normal and at oblique incidence. For the case of oblique incidence it is necessary to use a polarizer as shown in Fig. 1(b). The polarizer should select either p- or s-polarized light depending on the measurement requirements.

A typical spectral transmittance of the system at normal incidence is shown in Fig. 1(c). It consists of an 80-layer DM as the sample, a 10-μm air spacer, and a partially-transmitting Al mirror having virtually zero GDD, which closes the Fabry-Perot cavity. The reflection mode uses the same setup, but analyzes the reflected signal. The reflectance features sharp transitions between local maximum and minimum values (Fig. 1(d)). The reflectance is measured from the side of the metal mirror as shown in Fig. 1(b) at the normal incidence.
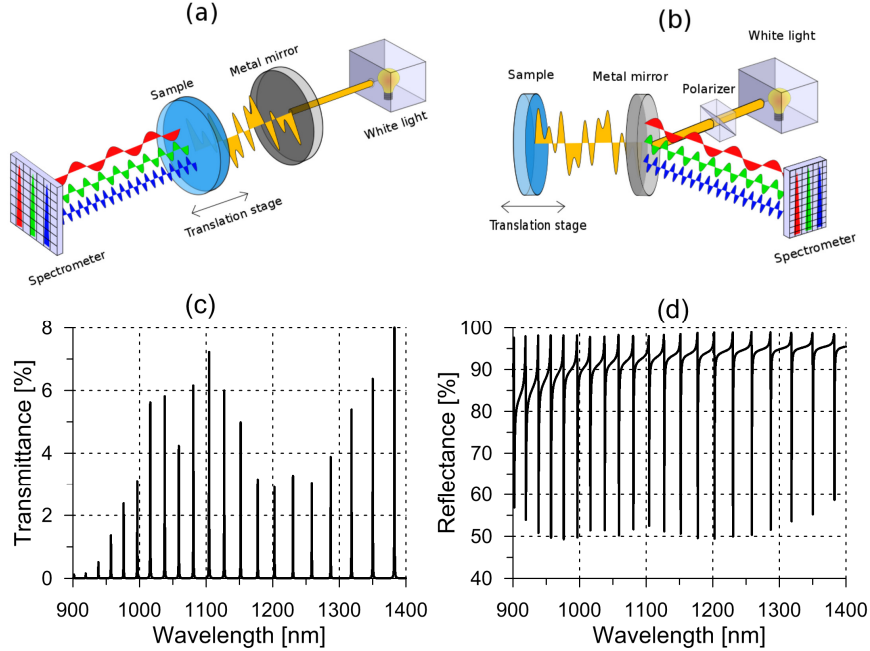

Fig. 1. Measurement setup for transmission mode (a) and for reflection mode (b) (the distance between mirrors is exaggerated). Simulated transmittance peaks (c) and reflectance resonances (d) for the system consisting of a 80-layer DM, 10- μm air spacer, and a partially-transmitting Al mirror having virtually zero GDD.

The total throughput (transmittance) of the system in the transmission mode can be expressed as [31]:

$$T = \frac{T_m T}{[1-(R_m^- R^+)^{1/2}]^2}\left[1+\frac{4(R_m^- R^+)^{1/2}}{[1-(R_m^- R^+)^{1/2}]^2}\sin^2\left(\frac{\varphi_m + \varphi}{2}-\delta\right)\right]^{-1}, \qquad (1)$$

where

$$\delta = \omega d_s n_s \cos\theta_s / c. \qquad (2)$$

Here T_m and T are transmittances of the metal mirror and the sample mirror respectively, R_m^-, R^+ are the reflectances of the metal mirror from the direction of light incidence and the opposite direction, respectively. φ_m and φ are the phase shifts imposed upon reflection off these mirrors, and δ is the phase shift associated with propagation

through the spacer of refractive index n_s and thickness d_s. The symbols θ_s, ω, and c represent the angle of incidence, the angular frequency and the phase velocity of the incident light wave, respectively.

Positions of the transmittance peaks are determined by the resonance condition:

$$\frac{\varphi_m + \varphi}{2} - \delta = \pi k, \quad k = 1,\ldots \qquad (3)$$

where k is integer and corresponds to the resonance order.

We will consider either transmittance maxima positions for the transmission mode (Fig. 1(a)) or reflectance minima positions for the reflection mode (Fig. 1(b)). Consider two adjacent resonance peaks located at angular frequencies ω_j and ω_{j+1}. The respective spectral variation of the phase shift imposed by the sample mirror upon reflection can be expressed as

$$\Delta\varphi_j \equiv \varphi_{j+1} - \varphi_j = \frac{2d_s n_s \cos\theta_s}{c}(\omega_{j+1} - \omega_j) - 2\pi. \qquad (4)$$

From this, by using $GD(\omega) = -d\varphi/d\omega$ we obtain:

$$\langle GD \rangle_j = -\frac{2d_s n_s \cos\theta_s}{c} + \frac{2\pi}{\Delta\omega_j}, \quad \Delta\omega_j = \omega_{j+1} - \omega_j, \qquad (5)$$

where $\langle GD \rangle_j = 1/\Delta\omega_j \int_{\omega_j}^{\omega_{j+1}} GD(\omega)d\omega$ is the average GD within the interval $\omega \in [\omega_j, \omega_{j+1}]$..

The spacer thickness d_s in Eq. (5) (i.e., the distance between mirrors) can be hardly determined with the necessary angstrom precision. Therefore it will be useful to exclude the spacer thickness from further considerations. This can be done in the following way: if two neighboring frequency intervals $\omega \in [\omega_j, \omega_{j+1}]$ and $\omega \in [\omega_{j+1}, \omega_{j+2}]$ are considered, the following relation between averaged GD values can be easily obtained:

$$\langle GD \rangle_{j+1} - \langle GD \rangle_j = 2\pi\left(1/\Delta\omega_{j+1} - 1/\Delta\omega_j\right). \qquad (6)$$

This relation is considered as a recurrent formula allowing to obtain averaged values of GD consequently for each interval. Since a constant additive term of GD is irrelevant, it is possible to use $\langle GD \rangle_0 = 0$ as an initial condition. In contrast to the relevant formulas [30], Eqs. (6) are not approximate; they deliver the spectrally averaged values of the group delay as accurately as the positions of the transmittance peaks are known. Therefore, Eq. (6) can be used with an arbitrary step size $\Delta\varphi_j$ and for any spacer thickness.

If the distance between two adjacent resonant peaks is small, the averaged GD values $\langle GD \rangle_j$ can be considered as a representation of the $GD(\omega)$ spectral dependence. Unfortunately the grid ω_j is not arbitrary; it is determined by the positions of resonant peaks. By increasing the thickness of the cavity it is possible to achieve a rather dense distribution of the peaks, but the amplitude of the peaks is decreasing rapidly and the peaks become masked by the noise of the measurement system. Even if peaks of small amplitude can be detected against the noise background, their positions may be highly affected by the noise and the direct application of Eq. (6) leads to unacceptably high errors. When the amplitude of resonance peaks is sufficient for accurate determination of their positions, they are spaced too sparsely for measuring GD and GDD spectral dependencies with nanometers resolution that modern applications demand.

3. Experimental procedures and numerical data analysis

In order to increase the density of the frequency grid we propose an alternative approach based on measurements with different spacer thicknesses and combined processing of all data sets. A similar idea was used in [32] to obtain a high precision phase reconstruction algorithm for extracting the spectral phase from interferograms taken at an arbitrary number of different shears.
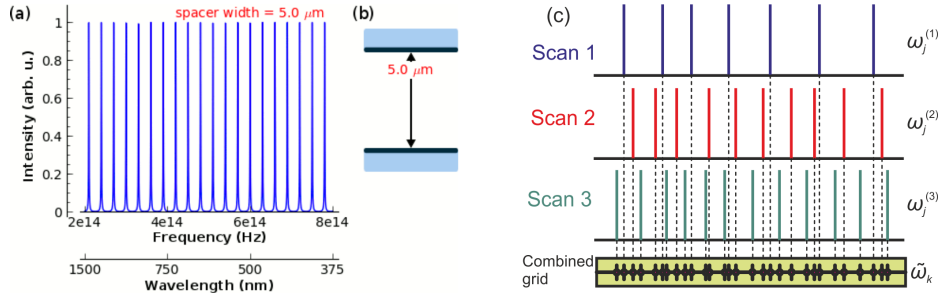

Fig. 2. Single-frame excerpt from video recording (Media 1) of resonance positions changes (a) with spacer thickness (b). Joining data from the measurements with different spacer thicknesses into a combined grid for data processing (c).

Simultaneous processing of data obtained from measurement scans with different spacer thicknesses can improve the spectral resolution (Figs. 2(a) and 2(b), multimedia file Media 1) of the method, since the density of the combined frequency grid will be significantly higher (Fig. 2(c)). It is possible to express terms $\langle GD \rangle_j$ in Eq. (6) through averaged GD values $\langle \widetilde{GD} \rangle_k$ over elementary combined grid intervals $\omega \in [\tilde{\omega}_k, \tilde{\omega}_{k+1}]$, $k = 1, \ldots, M-1$, where M is the total number of detected peaks for all measurement scans. Therefore Eqs. (6) can be reduced to a system of linear algebraic equations (SLAE) with respect to vector $\mathbf{b}$ with components $b_k = \langle \widetilde{GD} \rangle_k$:

$$\mathbf{Ab} = \mathbf{u} \qquad (7)$$

with the right-hand side $\mathbf{u}$ formed of right-hand sides of Eq. (6) and the matrix $\mathbf{A}$ obtained in accordance with relations of intervals of the combined grid $[\tilde{\omega}_k, \tilde{\omega}_{k+1}]$ and intervals of every measurement scan. The number of equations in the SLAE is less than the number of unknowns, since spacer thicknesses have been excluded during derivation of Eq. (6), therefore the SLAE is an under-determined one. This is a typical inverse ill-posed problem [33] that requires the so-called regularization theory [33,34] to be applied to find its solution.

The general approach described above has two shortcomings. The first one is related to the potentially high non-uniformity of the combined frequency grid. By accident there might be areas not covered densely enough with resonance peaks or, on the other hand, there might be areas with very high concentration of peaks collected from different measurement scans. This makes the condition number of the matrix $\mathbf{A}$ in the problem Eq. (7) higher and the solution of Eq. (7) more difficult. The second problem relates to the need for computing the GDD as a derivative of the GD spectral dependence, which is represented as a set of averaged $\langle \widetilde{GD} \rangle_k$ values on a combined essentially non-uniform grid $\tilde{\omega}_k$. Since averaged GD values are known only approximately, it requires additional application of numerical differentiation procedures that also belong to the class of ill-posed problems and require the application of the regularization theory and its corresponding algorithms [33].

In order to avoid these deficiencies we developed an approach based on the representation of the GD spectral dependence as a cubic spline function. Let us introduce a new frequency

grid x_i, $i = 0, \ldots, N$, that can be, for example, a uniform grid. Starting and ending points of this grid should coincide with the combined grid starting and ending points (Fig. 2): $x_0 = \tilde{\omega}_0$, $x_N = \tilde{\omega}_{M-1}$. Let us consider a cubic spline [35] defined by coefficients a_i, b_i, c_i, and d_i:

$$GD(\omega) = a_i + b_i(\omega - x_i) + c_i(\omega - x_i)^2 + d_i(\omega - x_i)^3, \quad \omega \in [x_i, x_{i+1}). \qquad (8)$$

The usual requirements are that $GD(\omega)$, $GD'(\omega)$, and $GD''(\omega)$ are continuous and the boundary conditions are $GD''(x_0) = GD''(x_N) = 0$. The set of basic Eqs. (6) after substitution of the expression Eq. (8) can be also rewritten as a SLAE having formally the same form like Eq. (7). In this case the vector $\mathbf{b}$ consists of the spline coefficients a_i, b_i, c_i, d_i. Depending on the total number of detected peaks in all scans M and the number of spline grid points N the SLAE can be over- or under-determined and the solution of this SLAE also requires application of the regularization theory [25]. The advantage of the spline-based approach reveals itself in the smaller condition numbers of the matrix $\mathbf{A}$, leading to better quality of obtained solutions. Since the first derivative of the spline Eq. (8) is a continuous smooth function, there are no difficulties in obtaining $GDD(\omega) = dGD(\omega)/d\omega$.
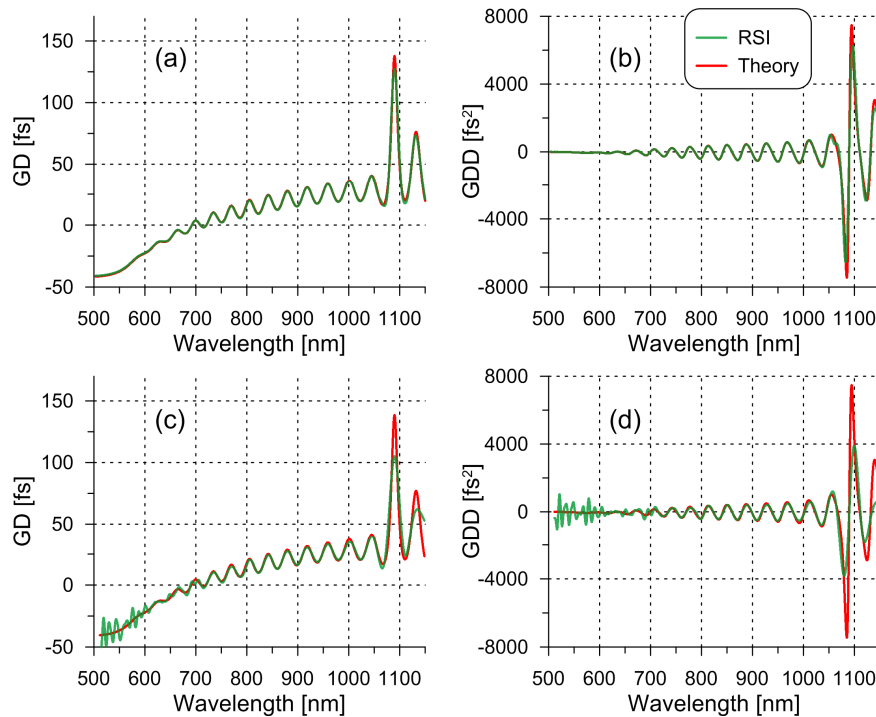

Fig. 3. Results of GD and GDD reconstruction in case of location of reflectance minima with a high accuracy (0.002 nm) ((a) – GD and (b) – GDD) and in case of a typical CCD spectrometer accuracy of 0.37nm ((c) – GD and (d) – GDD).

In order to confirm the accuracy and reliability of the proposed data processing technique we performed numerical experiments, in which we simulated the reflectance of a system consisted of an 80-layers broadband dispersive mirror, air spacer with thickness, which varied from 3 μm to 30 μm and a metal Al mirror with thickness 20 nm. We simulated ten measurement scans corresponding to air spacer thicknesses of 3, 5, 7, 10, 12, 15, 17, 20, 25, 30 μm. Since layer thicknesses of the 80-layer broadband dispersive mirror were known, the theoretical GD and GDD spectral dependencies were also known.

In the first numerical experiment we calculated the reflectance of the resonance system at an extra-fine grid with step size 0.002 nm. The resulting GD and GDD are shown with green curves (RSI) in Figs. 3(a) and 3(b), respectively. The theoretical GD and GDD are shown with red curves in these figures. Only small deviations of GDD can be noticed on the regions with high GDD oscillations, they appear because the regularization technique is assuming smoothness and oscillations with limited amplitude in GD and GDD functions as *a priori* information.

In the second numerical experiment we calculated the reflectance with wavelength step size 0.37 nm, which corresponds to the resolution of the CCD spectrometer used in our setup. The obtained results are represented in Fig. 3(c) (GD) and Fig. 3(d) (GDD). In order to refine the positions of detected peaks we used additional parabolic interpolation procedure. Nevertheless, the influence of inaccuracies can be noticed in Fig. 3(c) and Fig. 3(d) in the short wavelength region as artifact oscillations of the corresponding spectral dependencies. Here we should note that in this numerical example we considered a challenging measurement problem when a waveband of interest spanned about one optical octave, and the corresponding spectral dependencies had a complicated shape with high amplitude of oscillations.

The accuracy of the developed approach depends on a large number of various factors including the experimental setup and measurement strategy. Furthermore, we reduced data processing problem to an ill-posed SLAE Eq. (7) that requires a regularization theory in order to be solved [33]. In the theory of ill-posed problems a priori estimation of accuracy in practically significant cases is rarely available. Therefore we suggest using a method of model problems in order to estimate the accuracy. Typically the experimenter knows the theoretical design of DM sample, and therefore it is possible to perform a numerical experiment reproducing the experimental setup and measurements settings using an approach similar to the two numerical experiments described above. If the parameters of numerical experiments are close to the real parameters, it will give a good estimation of the expected accuracy of the obtained GD and GDD values. Such numerical experiments can include most of the factors affecting accuracy in reality: noise in spectrophotometer, finite size of wavelength grid, averaging due to spectrometer slit integration, etc.

4. Measurements

The measurement setup includes a light source, a spectrometer, and a translation stage (Fig. 1). We have used a grating spectrometer and different light sources and cameras for different spectral ranges. In our measurements at wavelengths above and below 450 nm we have drawn on a 250-Watt tungsten-halogen and a 75-Watt Xe lamp, respectively. A CCD camera (wavelength grid step of about 0.37 nm) and an InGaAs photodiode array (wavelength grid step of about 0.61 nm) detected the signal below and above 1050 nm, respectively. The mirror holder for the sample was mounted on a linear translation stage (step size: 0.1 μm), allowing us to vary the spacer thickness without affecting the initial alignment of mirrors. Therefore we were able to perform multiple measurements of positions of transmittance maxima or reflectance minima with different spacer thicknesses. We will call a single measurement of peak positions at some fixed spacer thickness a measurement scan. By averaging the data during every measurement scan the signal-to-noise ratio was significantly improved. It was sufficient to use short averaging time in the range 20-120 seconds. All measures were taken to keep the spacer thickness constant during each measurement, therefore Eq. (6) was assumed to be valid for each measurement scan. With typical number of scans about 10 total measurement time is approximately 15-20 minutes. With a typical number of about 10 scans the total measurement time was approximately 15-20 minutes.

The GD/GDD results for Examples 4.1 and 4.4 described below were compared with the results obtained with WLI. In our case WLI was based on the same light sources and CCD camera/InGaAs photodiode array that we used for RSI measurements. This gives us confidence to state that the comparison between RSI and WLI was fair.

4.1. Wideband dispersive mirror

As a first example we present the results of measurement data processing for a 98-layer wideband dispersive mirror in the range 600-1050 nm. Since this mirror transmits sufficient amount of light and provides a good signal-to-noise ratio, it is possible to perform measurements in both transmittance and reflectance configurations. Therefore we have performed both studies and obtained results.
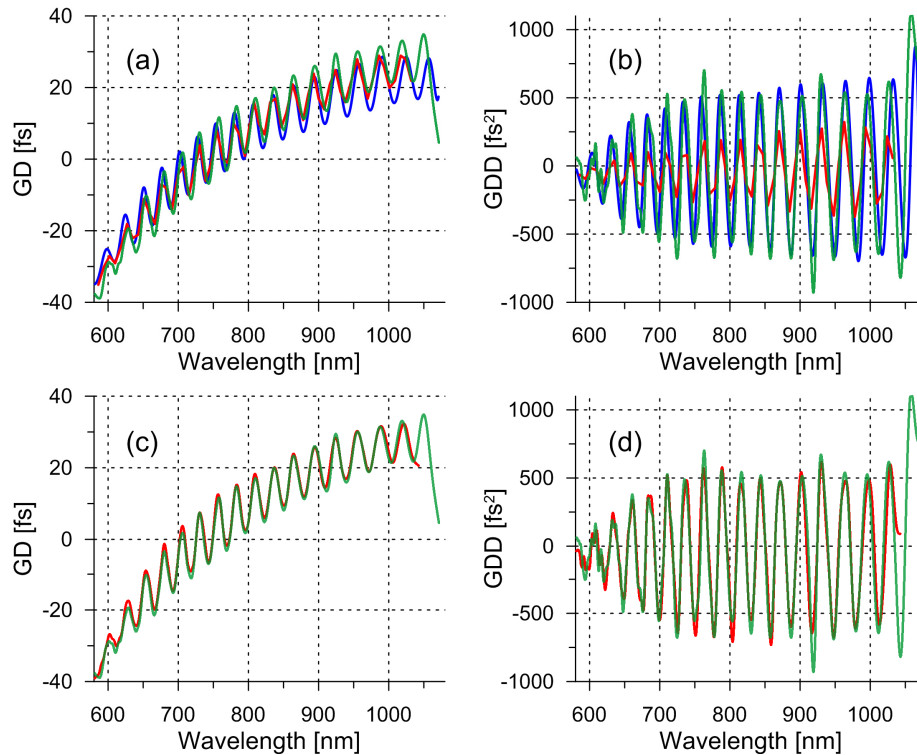

Fig. 4. GD (a) and GDD (b) obtained with RSI in transmittance mode (green curves), WLI results (red curves) and theoretical data (blue curves). Comparison of GD (c) and GDD (d) results obtained with RSI in transmittance mode (green curves) and in reflectance mode (red curves).

Figures 4(a)–4(b) present the GD and GDD evaluated from transmittance measurements (green curves). The measurements were performed with exposure time of 150 ms, 1000 spectra were used during each scan in order to improve the signal-to-noise ratio. A total number of 13 measurement scans with different spacer thicknesses were processed to obtain the GD and GDD spectral dependencies. They are compared with the results of WLI measurements (red curves) and with theoretical predictions (blue curves). It should be noted that deviations of measured GD and GDD from the theoretical ones were expected, since experimental GD and GDD were affected by unavoidable layer thickness errors and other perturbing factors in the manufactured mirrors. The spectral GD and GDD dependencies obtained by the RSI technique show much higher resolution and accuracy in comparison to WLI data. Additional verification of these results is provided in Fig. 4(c) and Fig. 4(d), where we compare GD and GDD obtained by using transmittance (green curves) and reflectance (red curves) measurements. Reflectance measurements were performed with exposure time of 25 ms, 500 spectra were averaged for every scan, in total 11 scans were processed. The results from completely different measurement sets, using different experimental layouts demonstrate a remarkable consistency.

4.2. Ultra-broadband (octave-spanning) dispersive mirror

The next example demonstrates simultaneous processing and analysis of measurement scans performed in different wavelength regions. In this case we consider an ultra-broadband 96-layer dispersive mirror with working range of 650-1350nm. Access to the entire spectral range of interest was not possible with a single measurement setup; therefore we split the wavelength band into two overlapping parts: 650-1060 nm and 850-1350 nm (covered by the CCD camera and the InGaAs photodiode array, respectively). We used exposure time of 50 ms and averaged 1000 spectra during each scans; in total we performed 22 scans with different spacer thicknesses (11 scans for each band).
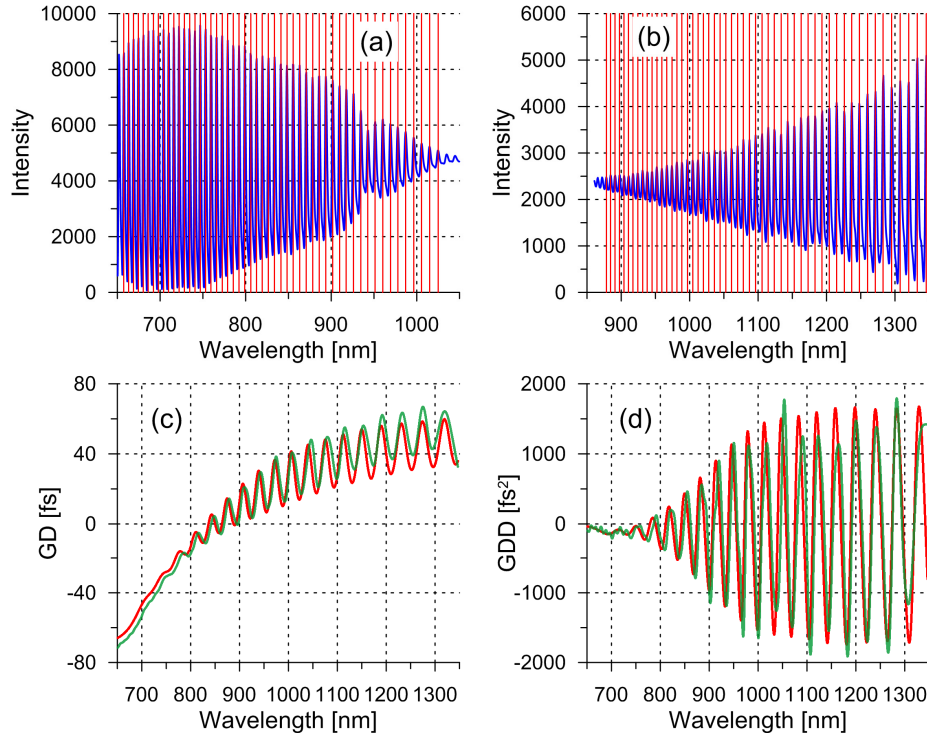

Fig. 5. Result of a typical reflectance scan (blue curves) in the ranges 650-1060 nm (a) and 850-1350 nm (b). Red vertical lines indicate positions of reflectance peaks. Measured data is represented in intensity non-normalized units. Obtained GD (c) and GDD (d) of the ultra-broadband 96-layer mirror (green curves) and theoretical data (red curves) for comparison.

In Fig. 5(a) and Fig. 5(b) we present two measurement sets for ranges 650-1060 nm and 850-1350 nm, respectively. The pronounced variation of the peak values of reflectance with wavelength is mainly due to a variation of the spectral response of our measurement system, which is operated here near the edge of the working range of our spectrometer. We performed simultaneous processing of all measurement scans in both wavelength regions, yielding the GD and GDD spectral dependencies shown in Fig. 5(c) and Fig. 5(d). These results demonstrate good correspondence with the respective theoretical predictions.

4.3. Ultraviolet dispersive mirror

Measurements and data processing were more complicated in the short wavelength region in comparison to visible and infrared regions, because the relative accuracy of determination of peak positions in the ultraviolet domain was lower with respect to longer wavelength regions. This is caused by higher ratio of the wavelength step between spectrometer pixels to the average wavelength. Such inaccuracies typically lead to artificial oscillations in GD and

especially in GDD spectral dependencies as it was demonstrated in the numerical simulation example (Fig. 3(c) and Fig. 3(d)).
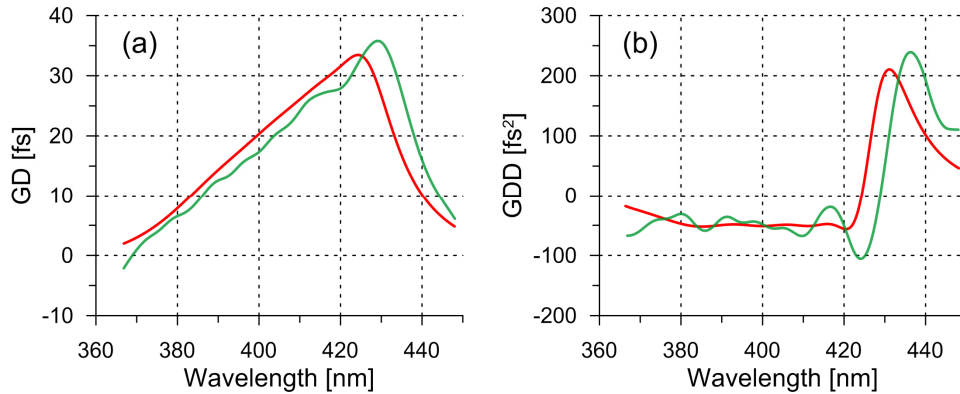

Fig. 6. GD (a) and GDD (b) evaluated from reflectance measurements for a mirror working in the ultraviolet (green curves) along with the corresponding theoretical predictions (red lines).

In spite of these difficulties, we have succeeded in performing measurements with reasonable accuracy also in the ultraviolet spectral range. Specifically, we characterized a 36-layer ultraviolet dispersive mirror working at angle of incidence of 45° and within the spectral range of 370-420 nm. In this case we employed the 75 Watt xenon lamp along with the CCD spectrometer; additionally a polarizer had to be used because of the large angle of incidence. We used 50 ms exposure time and averaged 1000 spectra for each measurement scan, a total number of 11 scans with different spacer thicknesses were processed. In Fig. 6 some shift of spectral characteristics to longer wavelengths can be noticed. Yet again, it can be attributed to manufacturing errors caused by a slight over-deposition of the mirror layers; the experimental results show excellent qualitative and quantitative agreement with theory (Fig. 6).

4.4 High-dispersion mirror

For mirrors exhibiting very high (near 100%) reflectance, measurements of GD and GDD are only possible in the reflection mode (Fig. 1(b)). We consider a high-dispersive mirror [9,27] with working range 1015-1030 nm, a nominal GDD of about -3000 fs^2, and a reflectance higher than 99.95% in this range. The latter makes the transmitted signal indistinguishable from noise. We characterized this DM in the range of 940-1100 nm in the reflection mode. In this case 300 spectra were averaged for each scan with exposure time of 300 ms, we processed 9 scans with different spacer thicknesses. Our results are shown in Figs. 7(a) and 7(b). The values of GD and GDD evaluated by using the RSI technique are compared with results of WLI measurements as well as with theoretical predictions. The resonant features positioned at about 960 and 1080 nm have been well reconstructed in the measured data (see Figs. 7(a) and 7(b)), while the WLI measurements have clearly failed to detect them. A slight shift of the measured curve to shorter wavelengths should be attributed to slight under-deposition of DM layers during the production process.

In order to gain more detailed insight into the working range of this DM, we performed an additional data processing of the same data constrained within the range 1000-1050 nm. The obtained results are presented in Figs. 7(c) and 7(d) for GD and GDD, respectively. One can notice the same shift of GD and GDD characteristics to shorter wavelengths. It is obvious that the new method has much higher spectral and GD/GDD resolutions compared to WLI. The oscillations in calculated GDD spectral dependence (Fig. 7(d)) should be attributed to unavoidable errors in DM layer thicknesses introduced during DM production.
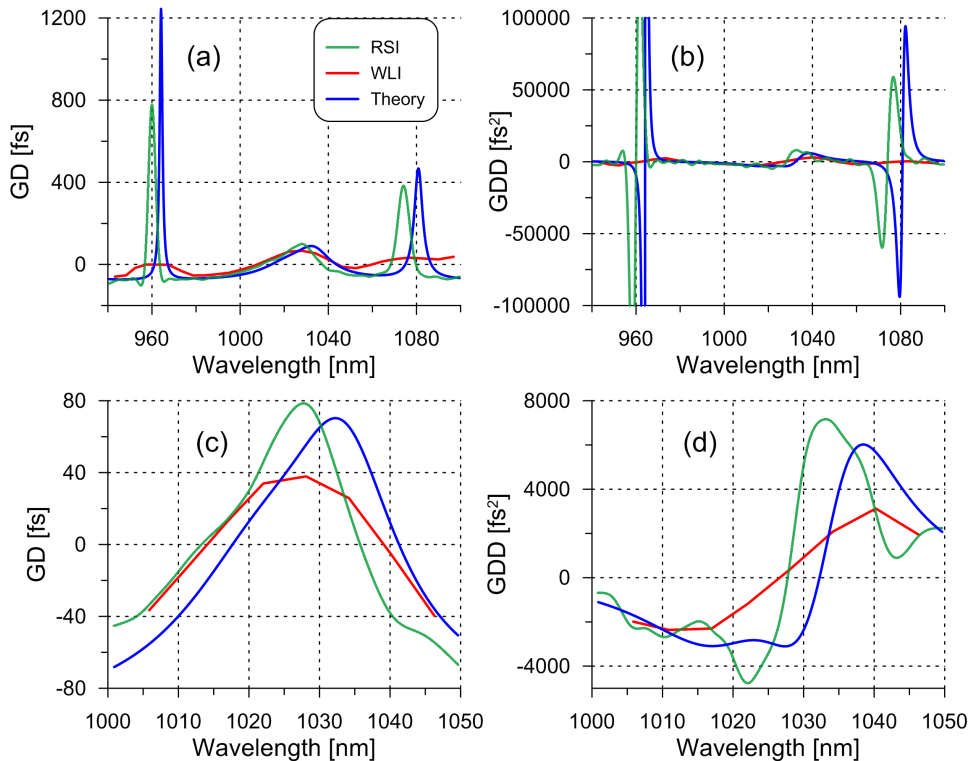
Fig. 7. GD (a, c) and GDD (b, d) RSI measurements for a high-dispersive mirror in a wide band 940-1100 nm (a, b) and in working range 1000-1040 nm (c, d) (green curves). Blue curves correspond to the theoretical GD and GDD, red curves – to WLI measurements.

5. Conclusions

We have proposed and demonstrated a Resonance Scanning Interferometer (RSI) technique for high-resolution and high-fidelity measurement of GD and GDD of multilayer optics. RSI draws on the basic interferometric concept originally proposed in [30] implemented simultaneously with a number of different separations of the mirrors forming the interferometer. The method can be carried out by processing and analyzing either transmitted or reflected signals from the interferometer and does not rely on an accurate measurement of the mirror separation. GD and GDD are evaluated from the measured data by using a versatile and powerful algorithm based on solving an inverse ill-posed problem. The demonstrated technique is expected to become instrumental in the development of advanced dispersive multilayer optics.